

# Multiple Queries with Multiple Keys: A Precise Prompt Matching Paradigm for Prompt-based Continual Learning

Dunwei Tu<sup>1,2</sup> Huiyu Yi<sup>1,2</sup> Yuchi Wang<sup>1,2</sup> Baile Xu<sup>1,2</sup> Jian Zhao<sup>3</sup> Furao Shen<sup>1,2</sup>

## Abstract

Continual learning requires machine learning models to continuously acquire new knowledge in dynamic environments while avoiding the forgetting of previous knowledge. Prompt-based continual learning methods effectively address the issue of catastrophic forgetting through prompt expansion and selection. However, existing approaches often suffer from low accuracy in prompt selection, which can result in the model receiving biased knowledge and making biased predictions. To address this issue, we propose the Multiple Queries with Multiple Keys (MQMK) prompt matching paradigm for precise prompt selection. The goal of MQMK is to select the prompts whose training data distribution most closely matches that of the test sample. Specifically, Multiple Queries enable precise breadth search by introducing task-specific knowledge, while Multiple Keys perform deep search by representing the feature distribution of training samples at a fine-grained level. Experiments show that MQMK enhances the prompt matching rate by over 30% in challenging scenarios and achieves state-of-the-art performance on three widely adopted continual learning benchmarks. Once this paper is accepted, we will release the code.

## 1. Introduction

Neural networks have become one of the most important models in the field of machine learning (Rumelhart et al., 1986; LeCun et al., 1998; Graves & Graves, 2012). In real-world scenarios, data may not always be fully accessible

<sup>1</sup>National Key Laboratory for Novel Software Technology, Nanjing University, China <sup>2</sup>School of Artificial Intelligence, Nanjing University, China <sup>3</sup>School of Electronic Science and Engineering, Nanjing University, China. Correspondence to: Dunwei Tu <tudunwei@smail.nju.edu.cn>, Yuchi Wang <yuchi.wang@smail.nju.edu.cn>, Furao Shen <frshen@nju.edu.cn>.

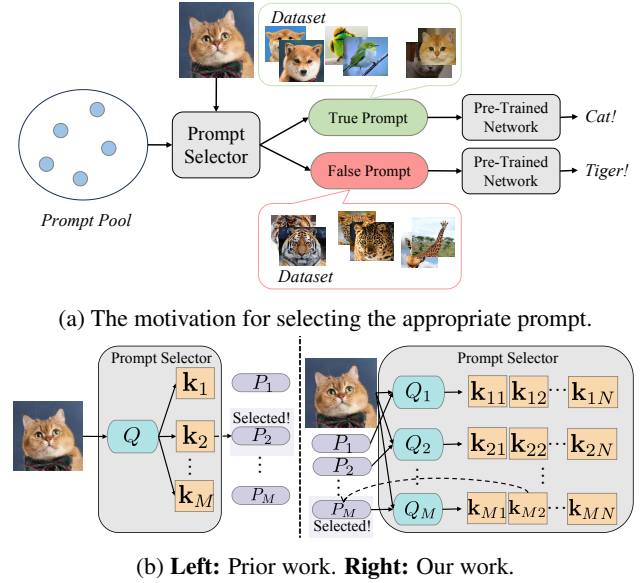


Figure 1. (a) Prompts with discrepancies between the training dataset and test samples may provide biased knowledge, leading to biased outputs. (b) Prior prompt selector uses a single query for all tasks and task-level keys. Our prompt selector uses task-level breadth queries and class-level depth keys. In our work, the prompts are involved in the prompt selection process, whereas prior work does not include these.

from the start, and the dynamic nature of the world continuously introduces new data. This requires neural networks to possess the ability for continual learning (Belouadah et al., 2021; Zhou et al., 2024; De Lange et al., 2021), in order to maintain knowledge updates and adapt to new environments. Additionally, humans do not forget old knowledge when learning new knowledge, making continual learning a key technology for building artificial intelligence that mirrors human learning.

In the context of continual learning, the data across different learning tasks is often non-independent and identically distributed (non-i.i.d.). Non-i.i.d. data requires the model to continuously adjust its parameters based on new data in order to establish decision boundaries that are more suited to the current data. However, this adaptation can lead to the

forgetting of previously learned knowledge. Some studies suggest that unless certain measures are taken, the neural network’s ability to recognize previously encountered classes inevitably deteriorates during the learning process for new tasks, a phenomenon known as catastrophic forgetting (Nguyen et al., 2019; McCloskey & Cohen, 1989; McClelland et al., 1995).

Early continual learning methods design sustainable learning from aspects such as parameters (Kirkpatrick et al., 2017; Li & Hoiem, 2017), data (Rebuffi et al., 2017; Shin et al., 2017), gradients (Lopez-Paz & Ranzato, 2017; Mirzadeh et al., 2020), features (Madaan et al., 2021; Pham et al., 2021), and architecture (Yan et al., 2021; Wang et al., 2022a), training a neural network from scratch, which has yielded promising results. Recent continual learning algorithms (Zhou et al., 2024; Wang et al., 2022c; McDonnell et al., 2024) have started to focus on how to use pre-trained models for continual learning, aiming to leverage the strong generalization ability of pre-trained models to adapt to dynamic downstream tasks.

The prompt-based methods (Wang et al., 2022b;c; Smith et al., 2023; Jung et al., 2023; Gao et al., 2024; Kurniawan et al., 2024), as emerging pre-trained model based approaches, counter the forgetting problem and make reasonable use of the generalization knowledge of pre-trained models in a clever manner. These methods utilize a frozen backbone network, such as Vision Transformer (ViT) (Dosovitskiy, 2020), pre-trained on a large-scale dataset like ImageNet (Russakovsky et al., 2015), and adapt the model to downstream continual learning tasks through Visual Prompt Tuning (VPT) (Jia et al., 2022). A major advantage of these approaches is that task-specific knowledge can be stored in the form of prompts, and as tasks increase, the prompts are continuously expanded, thereby forming a prompt pool that encompasses all the knowledge learned by the model.

Prompts can be learned using VPT techniques on different tasks. However, a key question is how to select the appropriate prompt for inference. Existing methods (Wang et al., 2022c;b) employ a query-key matching mechanism for prompt selection. Specifically, this approach uses a pre-trained ViT without prompts as the query function and employs task-specific, learnable parameters as the key for the prompt retrieval. However, a key issue is that the matching mechanism is not sufficiently precise. A prompt trained on an inconsistent data distribution with the test samples may not be effective in assisting inference, as shown in Figure 1a. From the results, improving the matching rate can effectively boost model performance (see Section 3.3).

To improve the matching rate and the consistency between the prompt and the test samples, we propose the Multiple Queries with Multiple Keys (MQMK) matching paradigm. Unlike the current Single Query-Single Key

(SQSK) paradigm, where a single query matches a single key (Wang et al., 2022c;b; Smith et al., 2023), our method extends the queries across all tasks and forms a query pool, with each query corresponding to a task, as shown in Figure 1b. This query pool, which includes all task-specific prompts and contains task-related knowledge, is used for task-level breadth search. And during the process of key and query matching, the prompts are involved, thereby establishing a direct connection between the keys and the prompts. Therefore, it is more accurate than a single query solely based on the features of a pre-trained model. Additionally, we extend the original task-level keys to Multiple Keys in each task to better represent the feature distribution of the training samples for deep search. Our experiments demonstrate that the performance is optimal when Multiple Keys are extended to the class level. Through horizontal expansion of the query-key matching mechanism, the MQMK paradigm significantly improves the matching rate, achieving 32.82% improvement in certain scenario, and delivers State-Of-The-Art (SOTA) performance across three challenging and well-recognized continual learning datasets. Our method and experiments provide strong evidence that, in addition to improving prompt quality, directly enhancing the matching mechanism can effectively improve performance.

The contributions of this paper are summarized as follows:

1. For the first time, we discuss the importance of query-key matching rate in improving model performance in prompt-based methods, defining current approaches as the Single Query-Single Key (SQSK) paradigm and introducing the Multiple Queries with Multiple Keys (MQMK) paradigm, which achieves an improvement of 32.82% in matching rate and reaches SOTA performance.
2. We identify that the SQSK paradigm lacks prompt information in the query, specifically task-specific knowledge, which leads to low query precision. Additionally, in SQSK, the prompt itself is not involved in the process of prompt selection. To address these, we extended the Single Query to Multiple Queries for task-level breadth search.
3. After introducing Multiple Queries, the feature gap between classes within a task becomes further pronounced. A single key can no longer represent the feature distribution of the training samples used for prompt optimization. Therefore, we extend the Single Key to Multiple Keys for deep search and find that the performance is optimal when the key granularity is at the class level.

## 2. Related Work

**Continual Learning.** Early continual learning methods can generally be classified into five categories: regularization-

based methods (Kirkpatrick et al., 2017; Li & Hoiem, 2017), replay-based methods (Rebuffi et al., 2017; Shin et al., 2017), optimization-based methods (Lopez-Paz & Ranzato, 2017; Mirzadeh et al., 2020), representation-based methods (Madaan et al., 2021; Pham et al., 2021), and architecture-based methods (Yan et al., 2021; Wang et al., 2022a). Regularization-based methods address the forgetting problem by adding explicit regularization terms to balance the old and new tasks. Replay-based methods design strategies to retain important old samples in order to preserve the model’s previous knowledge. Optimization-based methods aim to make the gradients of new and old tasks as independent as possible, avoiding interference in order to prevent forgetting. Representation-based methods enhance the compatibility with new knowledge through meta-learning (Finn et al., 2017; Ravi & Larochelle, 2017) and self-supervised learning (Chen et al., 2020). Architecture-based methods adapt to dynamic task objectives through dynamic networks.

**Prompt-based Continual Learning.** Prompt-based methods are a type of continuous learning method based on pre-trained models. They leverage task-specific knowledge from the prompt and the generalized knowledge from the pre-trained model, resulting in superior performance. L2P (Wang et al., 2022c) and DualPrompt (Wang et al., 2022b) introduce VPT into continual learning, where prompt vectors can be progressively expanded as tasks increase, thereby avoiding catastrophic forgetting caused by adjusting the same set of parameters for different tasks. L2P proposes a query-key matching approach for instance-wise prompt retrieval, while DualPrompt introduces general prompts to learn knowledge across tasks and provides general knowledge. CODA-P (Smith et al., 2023) introduces a decomposed attention-based prompt querying method, where prompts are combined with varying weights. ESN (Wang et al., 2023) addresses stage interference and performance imbalance by using stage-isolated classifiers, energy normalization, and voting-based inference. EvoPrompt (Kurniawan et al., 2024) addresses prompt selection mismatches and adaptive prompting challenges by using a dynamic, evolving prompt memory system that integrates reference and working prompts through optimal transport and bias adjustment. CPrompt (Gao et al., 2024) employs a random prompt selection training approach to address the issue of prompt inconsistency between training and testing phases.

### 3. Preliminaries

#### 3.1. Problem Setting

In our problem setting, we feed the model with a sequence of dataset  $\{\mathcal{D}_t\}_{t=1}^T$ , where  $\mathcal{D}_t$  is the dataset of the task  $t$  and  $T$  is the number of all tasks.  $\mathcal{D}_t = \{(\mathbf{x}_i, y_i)\}$  contains pairs of the sample  $\mathbf{x}_i$  and its corresponding label  $y_i$ . Each

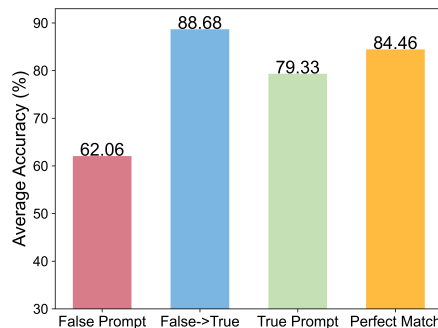


Figure 2. The average accuracy for four scenarios: when SQSK selects False Prompt and True Prompt, when samples initially with False Prompt are manually replaced with True Prompt, and when all samples use True Prompt.

task has a distinct label space, meaning that  $\mathcal{Y}^t \cap \mathcal{Y}^{t'} = \emptyset$  for any  $t \neq t'$ , where  $\mathcal{Y}^t$  represents the label space of task  $t$ . Moreover, once the model transitions to the next task, it cannot access any of the previous datasets. When there are test samples for inference, the model needs to make predictions based on the label spaces of all the tasks it has encountered. We do not provide the task ID of the sample to the model, making this a more challenging class-incremental continual learning (Chaudhry et al., 2018) setup.

#### 3.2. Model Tuning and Prompt Pool

Following previous prompt-based continual learning works (Wang et al., 2022c;b; Smith et al., 2023; Gao et al., 2024; Kurniawan et al., 2024), we use ViT as the backbone  $f = f_r \circ f_e$  and a single linear layer  $W$  as the classification head, where  $f_e$  is the embedding layer and  $f_r$  is the Multiple Self-Attention (MSA) layers. Given an image input  $\mathbf{x}$ , we first divide it into patches  $\mathbf{x}_p \in \mathbb{R}^{L \times (S^2 \times C)}$ , where  $L$  is the token length,  $S$  is patch size and  $C$  is the number of channels. And then pass them through  $f_e$  to obtain corresponding embeddings  $\mathbf{x}_e \in \mathbb{R}^{L \times D}$ , where  $D$  is embedding (token) dimension (768). Next, the embeddings  $\mathbf{x}_e$  and the prompt  $P$  are fed into  $f_r$  for feature extraction to obtain the output  $f_r(P; \mathbf{x}_e) \in \mathbb{R}^{L \times D}$ . The first token of the output,  $f_r(P; \mathbf{x}_e)[0] \in \mathbb{R}^D$ , which serves as the [class] token, is passed through the classification head  $W \in \mathbb{R}^{D \times |\mathcal{Y}^1 \cup \mathcal{Y}^2 \cup \dots \cup \mathcal{Y}^T|}$  to obtain the prediction, where  $|\mathcal{Y}^1 \cup \mathcal{Y}^2 \cup \dots \cup \mathcal{Y}^T|$  represents the total number of classes across all tasks.

To address catastrophic forgetting, L2P and DualPrompt design a paradigm where prompts expand with the tasks. Specifically, as tasks expand, the expert prompts (e-prompts) specific to each task and the general prompts (g-prompts) (Wang et al., 2022b) shared across tasks together form the prompt pool  $\mathbf{P} = \{P_g, P_1, P_2, \dots, P_M\}$ , where  $P_g \in \mathbb{R}^{L_g \times D}$  is the g-prompt,  $P_t \in \mathbb{R}^{L_e \times D}$  is the e-prompt of

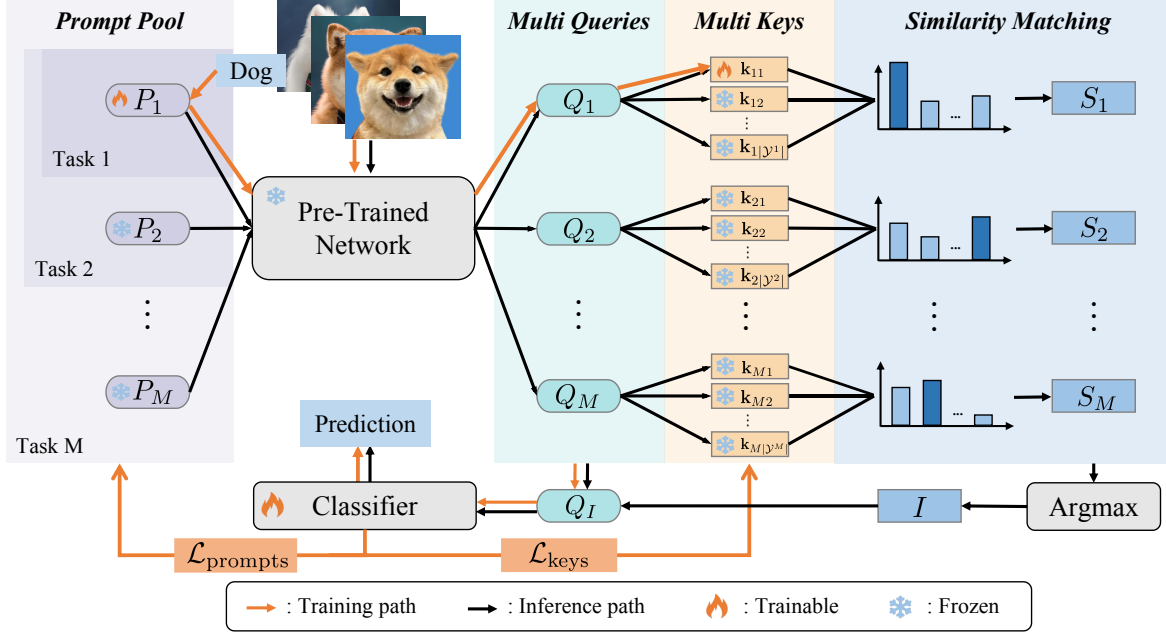


Figure 3. Overall pipeline of MQMK. **Training:** Directly selects the true prompt based on the label information and inputs it into the backbone to obtain the corresponding query for classification. This process updates the prompt, the key associated with the label and the classifier. **Inference:** Feeds each prompt into the backbone to generate the corresponding query and selects the most consistent query for classification by matching the task-level queries with the class-level keys.

$t$ -th task,  $M$  is the pool size,  $L_g$  is the length of g-prompt and  $L_e$  is the length of e-prompt. To retrieve prompts, they set a learnable parameter  $\mathbf{k}_t \in \mathbb{R}^D$  for the  $t$ -th e-prompt and form a prompt pool consisting of key-value pairs,  $\mathbf{P} = \{P_g, (\mathbf{k}_1, P_1), (\mathbf{k}_2, P_2), \dots, (\mathbf{k}_M, P_M)\}$ . The features extracted by the ViT without prompts,  $f_r(\mathbf{x}_e)[0] \in \mathbb{R}^D$ , are used as the query  $Q$ , and the prompt is selected by:

$$I = \underset{t \subseteq [1, M]}{\operatorname{argmax}} \cos(Q, \mathbf{k}_t), \quad (1)$$

where  $I$  represents the index of the selected prompt  $P_I$  and  $\cos(\cdot, \cdot)$  denotes cosine similarity function. Finally, the ViT, along with  $P_I$  and  $P_g$ , is used to classify the samples. Since each sample has only one  $Q$  and each  $P$  corresponds to one  $\mathbf{k}$ , we define this query paradigm as the Single Query-Single Key (SQSK) paradigm.

### 3.3. Prompt Matching Rate

We define the true prompt as a prompt that was trained on the task to which the sample belongs, i.e.,  $I = t$  for a sample  $(\mathbf{x}_i, y_i) \in \mathcal{D}_t$ , which means the sample’s distribution aligns with the distribution of the prompt’s training samples. Our experiments show that the matching rate under the SQSK paradigm is only 45.15% in 10-task Split ImageNet-R (Hendrycks et al., 2021). As shown in Figure 2, if the samples initially with False Prompt are manually replaced with True Prompt, the performance can be improved by

26.62%. Interestingly, the accuracy of the samples initially with False Prompt, after being replaced with True Prompt, is even higher than that of the samples initially with the True Prompt. This suggests that samples selected initially with the False Prompt not only require more task-specific knowledge, but also achieve a higher recognition rate once the true knowledge is incorporated.

## 4. Method

Our method uses the same model and tuning approach as SQSK, with the innovation of our method lying in the design of keys and queries, as well as their matching mechanism. The overall pipeline of our framework is illustrated in Figure 3.

### 4.1. The Design Goal

We aim to ensure that the test sample conforms to the distribution of the training samples used for prompt optimization, as this will enable the prompt to effectively handle the test sample. To achieve this goal, we need to address the following two questions:

1. How can we extract sample features for similarity judgment?
2. How can we represent the feature distribution of the samples used for prompt training?

For question 1, we employ a ViT with prompts as the query function. A ViT with prompts not only incorporates ViT’s generalized knowledge but also task-specific fine-grained knowledge, enabling more precise feature extraction for queries. For question 2, we introduce class-level learnable parameters as keys. Since samples within a class tend to be similar, class-level keys can represent the feature distribution of a task’s samples better. With queries and keys in place, the model can evaluate the similarity between the query and keys, selecting the most consistent prompt for the sample to make the final prediction.

## 4.2. Multiple Queries Matching Multiple Keys

We set  $|\mathcal{Y}^t|$  different learnable keys  $\mathbf{k}_t$  for  $P_t$ , where  $|\mathcal{Y}^t|$  denotes the number of categories in task  $t$ . The set of keys  $\mathbf{K}_t = \{\mathbf{k}_{t1}, \mathbf{k}_{t2}, \dots, \mathbf{k}_{t|\mathcal{Y}^t|}\}$  collectively performs retrieval for  $P_t$ , where  $\mathbf{k}_{tj}$  denotes the key for class  $j$  in task  $t$ . The keys and prompts together form a key-value pair pool:  $\mathbf{P} = \{P_g, (\mathbf{K}_1, P_1), (\mathbf{K}_2, P_2), \dots, (\mathbf{K}_M, P_M)\}$ . We refer to these keys, where a task contains multiple keys for deep search, as MK. MK was originally introduced by CPrompt (Gao et al., 2024), but in fact, our MK differs fundamentally from the MK in CPrompt. This distinction will be explained in detail in Section 4.3.

Given a sample  $\mathbf{x}$ , we use the  $t$ -th e-prompt and g-prompt in combination with ViT for feature extraction to obtain  $f_r(P_g; P_t; \mathbf{x}_e)[0]$ , which serves as the  $t$ -th query  $Q_t \in \mathbb{R}^D$ . The queries generated by using different e-prompts form a query pool  $\mathbf{Q} = \{Q_1, Q_2, \dots, Q_M\}$ . We refer to task-level queries for breadth search as MQ. Next,  $Q_t$  is matched with  $\mathbf{k}_{tj}$  by calculating the cosine similarity  $\cos\langle Q_t, \mathbf{k}_{tj} \rangle$ . At this point, each prompt has matching scores for all the categories within the task. We need to select the top- $K$  categories with the highest score within a task for aggregation by:

$$S^t = \max_{\{c_m\}_{m=1}^K \subseteq [1, |\mathcal{Y}^t|]} \sum_{m=1}^K \cos\langle Q_t, \mathbf{k}_{tc_m} \rangle, \quad (2)$$

where  $S^t$  is the aggregated matching score between the query and the  $t$ -th prompt. Finally, we select the highest matching score, and get the corresponding index as follows:

$$I = \operatorname{argmax}_{t \in [1, M]} S^t. \quad (3)$$

Finally, the model can make predictions according to the selected query  $Q_I$  and the linear classifier.

## 4.3. Optimization Objective

The overall optimization objective is divided into two parts: one is the learning of the prompts, and the other is the learning of the keys. The prompts are learned by optimizing the cross-entropy loss between the predicted results and the

ground truth by:

$$\mathcal{L}_{\text{prompts}} = \text{CE}(W^T f_r(P_g; P_t; \mathbf{x}_e)[0], y), \quad (4)$$

where  $\text{CE}(\cdot, \cdot)$  is cross-entropy function, and  $t$  is the task ID. During the training process, the task ID can be directly used to select the e-prompt.

Since queries have already been dispersed through cross-entropy in the classification objective, the objective for the keys is solely to align with the queries. Hence, the loss for learning the keys can be written as:

$$\mathcal{L}_{\text{keys}} = \sum_{i=1}^M \mathbb{I}(i = t) \sum_{j=1}^{|\mathcal{Y}^i|} (1 - \cos\langle Q_i, \mathbf{k}_{ij} \rangle) \mathbb{I}(j = y), \quad (5)$$

where  $\mathbb{I}(\cdot)$  is the indicator function. Our MK learns by aligning with the MQ that has already been dispersed through cross-entropy. In contrast, the MK in CPrompt learns by dispersing itself through cross-entropy, since SQ is fixed and not dispersed. Our MK is a component specifically adapted for MQ.

As shown in Equation (5), keys corresponding to other categories and queries corresponding to other prompt are not involved in the loss calculation. This means that during training, only one query is required, implying that the MQ mechanism not only does not introduce additional computational burden, but actually requires one less query without prompt compared to SQSK in the training process. The overall loss function can be written as:

$$\mathcal{L} = \mathcal{L}_{\text{prompts}} + \mathcal{L}_{\text{keys}}. \quad (6)$$

## 4.4. Discussion on Inference Computational Costs

MQ needs to be executed in the inference process, so  $M$  forward passes through the ViT backbone are required to obtain all queries. In contrast, SQSK only requires one query without the prompt and one prediction with the selected prompt. Therefore, the computational cost of MQMK is approximately  $M/2$  times that of SQSK. The different  $Q_t$  queries are independent of each other. Therefore, if computational resources are sufficient, the computation time of MQMK can be reduced to  $1/M$  of the original time. The is a theoretical analysis, and the practical results, the parameters analysis and computational costs during the training phase, are discussed in Appendix B.

# 5. Experiments

## 5.1. Evaluation Benchmarks

**Dataset.** We shuffle the classes and perform task splitting on three widely used visual datasets for prompt-based continual learning: CIFAR-100 (Krizhevsky et al., 2009), ImageNet-R (Hendrycks et al., 2021), and DomainNet (Peng et al.,

| Tasks               | 5                                  |                                   | 10                                 |                                   | 20                                 |                                   |
|---------------------|------------------------------------|-----------------------------------|------------------------------------|-----------------------------------|------------------------------------|-----------------------------------|
| Method              | $A_T$ ( $\uparrow$ )               | $F_T$ ( $\downarrow$ )            | $A_T$ ( $\uparrow$ )               | $F_T$ ( $\downarrow$ )            | $A_T$ ( $\uparrow$ )               | $F_T$ ( $\downarrow$ )            |
| joint train         | 79.27                              | -                                 | 79.27                              | -                                 | 79.27                              | -                                 |
| L2P++*              | 70.83 $\pm$ 0.58                   | 3.36 $\pm$ 0.18                   | 69.29 $\pm$ 0.73                   | 2.03 $\pm$ 0.19                   | 65.89 $\pm$ 1.30                   | 1.24 $\pm$ 0.14                   |
| Deep L2P++*         | 73.93 $\pm$ 0.37                   | 2.69 $\pm$ 0.10                   | 71.66 $\pm$ 0.64                   | 1.78 $\pm$ 0.16                   | 68.42 $\pm$ 1.20                   | 1.12 $\pm$ 0.13                   |
| DualPrompt*         | 73.05 $\pm$ 0.50                   | 2.64 $\pm$ 0.17                   | 71.32 $\pm$ 0.62                   | 1.71 $\pm$ 0.24                   | 67.87 $\pm$ 1.39                   | 1.07 $\pm$ 0.14                   |
| ESN $\ddagger$      | 73.42 $\pm$ 0.40                   | 3.79 $\pm$ 0.55                   | 75.11 $\pm$ 0.36                   | 5.68 $\pm$ 0.77                   | 70.57 $\pm$ 0.62                   | 6.84 $\pm$ 0.36                   |
| CODA-P*             | 76.51 $\pm$ 0.38                   | 2.99 $\pm$ 0.19                   | 75.45 $\pm$ 0.56                   | <b>1.64 <math>\pm</math> 0.10</b> | 72.37 $\pm$ 1.19                   | <b>0.96 <math>\pm</math> 0.15</b> |
| EvoPrompt $\dagger$ | 77.16 $\pm$ 0.18                   | 9.89 $\pm$ 0.30                   | 76.83 $\pm$ 0.08                   | 2.78 $\pm$ 0.06                   | 74.41 $\pm$ 0.23                   | 2.56 $\pm$ 0.22                   |
| CPrompt $\ddagger$  | -                                  | -                                 | 77.14 $\pm$ 0.11                   | 5.97 $\pm$ 0.68                   | 74.79 $\pm$ 0.28                   | 7.34 $\pm$ 0.65                   |
| MQMK                | <b>79.61 <math>\pm</math> 0.27</b> | <b>1.59 <math>\pm</math> 0.26</b> | <b>78.36 <math>\pm</math> 0.35</b> | 2.24 $\pm$ 0.20                   | <b>75.13 <math>\pm</math> 0.22</b> | 3.16 $\pm$ 0.26                   |

Table 1. Results (%) on Split ImageNet-R under 5-task, 10-task and 20-task settings. Best results are marked in bold. All our results are over 5 trials. \*: Results from (Smith et al., 2023).  $\ddagger$ : Results from (Gao et al., 2024).  $\dagger$ : Results from (Kurniawan et al., 2024).

| Method              | $A_T$ ( $\uparrow$ )               | $F_T$ ( $\downarrow$ )            |
|---------------------|------------------------------------|-----------------------------------|
| joint train         | 91.79                              | -                                 |
| L2P++*              | 82.50 $\pm$ 1.10                   | 1.75 $\pm$ 0.42                   |
| Deep L2P++*         | 84.30 $\pm$ 1.03                   | <b>1.53 <math>\pm</math> 0.40</b> |
| DualPrompt*         | 83.05 $\pm$ 1.16                   | 1.72 $\pm$ 0.40                   |
| ESN $\ddagger$      | 86.42 $\pm$ 0.80                   | 6.08 $\pm$ 0.48                   |
| CODA-P*             | 86.25 $\pm$ 0.74                   | 1.67 $\pm$ 0.26                   |
| EvoPrompt $\dagger$ | 87.97 $\pm$ 0.30                   | 2.60 $\pm$ 0.42                   |
| CPrompt $\ddagger$  | 87.82 $\pm$ 0.21                   | 5.06 $\pm$ 0.50                   |
| MQMK                | <b>91.73 <math>\pm</math> 0.18</b> | <b>2.67 <math>\pm</math> 0.17</b> |

Table 2. Results (%) on Split CIFAR-100 under 10-task setting. Best results are marked in bold. All our results are over 5 trials. \*: Results from (Smith et al., 2023).  $\ddagger$ : Results from (Gao et al., 2024).  $\dagger$ : Results from (Kurniawan et al., 2024).

2019), in order to align with the problem setup and conduct comprehensive experiments. We divide CIFAR-100 and DomainNet into 10 tasks, while ImageNet is divided into three cases: 5 tasks, 10 tasks, and 20 tasks. The dataset introduction is in Appendix F. The data distributions of DomainNet and ImageNet-R differ significantly from the ImageNet dataset used for model pre-training. This requires the model to continually learn new knowledge from these datasets, rather than relying on the knowledge learned from the pre-training dataset.

**Evaluation Metrics.** Average accuracy (Kim & Han, 2023; Yan et al., 2021; Li & Hoiem, 2017) and forgetting rate (Chaudhry et al., 2018; Lopez-Paz & Ranzato, 2017) are the two core metrics we use.  $A_T$  is the average accuracy on tasks 1 to  $T$  after the model has learned task  $T$ , and can be computed by:

$$A_T = \frac{1}{T} \sum_{t=1}^T \text{Accuracy}(t, T), \quad (7)$$

where  $\text{Accuracy}(t, T)$  represents the accuracy on task  $t$  after learning task  $T$ .  $F_T$  is the average accuracy drop across all

| Method      | $A_T$ ( $\uparrow$ )               | $F_T$ ( $\downarrow$ )            |
|-------------|------------------------------------|-----------------------------------|
| joint train | 89.15                              | -                                 |
| L2P         | 81.17 $\pm$ 0.83                   | 8.98 $\pm$ 1.25                   |
| DualPrompt  | 81.70 $\pm$ 0.78                   | 8.04 $\pm$ 0.31                   |
| ESN         | 79.22 $\pm$ 2.04                   | 10.62 $\pm$ 2.12                  |
| CODA-P      | 80.04 $\pm$ 0.79                   | 10.16 $\pm$ 0.35                  |
| CPrompt     | 82.97 $\pm$ 0.34                   | 7.45 $\pm$ 0.93                   |
| MQMK        | <b>85.62 <math>\pm</math> 0.33</b> | <b>5.51 <math>\pm</math> 0.22</b> |

Table 3. Results (%) on Split DomainNet under 10-task setting. Best results are marked in bold. All our results are over 5 trials. Except for MQMK, all the other results come from (Gao et al., 2024).

tasks, and can be computed by:

$$F_T = \frac{1}{T} \sum_{t=1}^T (\text{Accuracy}(t, t) - \text{Accuracy}(t, T)). \quad (8)$$

Average accuracy directly reflects the overall performance of the model, while forgetting rate indicates the trend of performance change. Therefore, average accuracy is relatively more important.

**Implementation Details.** ViT-B/16 (Dosovitskiy, 2020) trained on ImageNet-1K (Russakovsky et al., 2015) is the backbone we use, so  $S$  is set to 16. G-prompt is used in the first two layers of MSA, with a length of 5. The depth and length of e-prompt are discussed in Section 5.5. In all experiments,  $M$  is set equal to  $T$ , meaning that only one prompt is learned for each task. Each prompt selects only the category with the highest similarity for aggregation which implies that  $K$  is set to 1. For both SQSK and MQMK, a learning rate of 0.005, a batch size of 64, and the Adam (Kingma, 2014) optimizer with  $\beta_1 = 0.9$  and  $\beta_2 = 0.999$  are used in all experiments.

**Competitors and Joint Training.** We compare our method with SOTA prompt-based continual learning models, including L2P (Wang et al., 2022c), DualPrompt (Wang et al.,

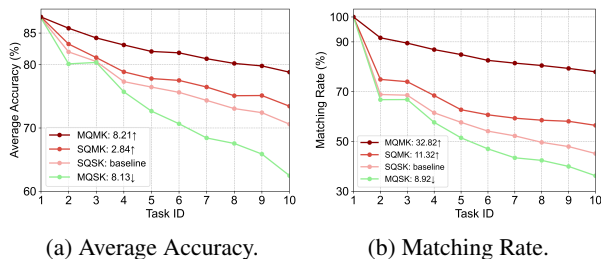


Figure 4. Ablation experiments on the 10-task Split ImageNet-R. The average accuracy and matching rate change with the learning process.

2022b), ESN (Wang et al., 2023), CODA-P (Smith et al., 2023), EvoPrompt (Kurniawan et al., 2024) and CPrompt (Gao et al., 2024). To ensure a fair comparison, we use SQSK as a baseline in some experiments. SQSK and MQMK have identical prompts, with the only difference being the matching mechanism. SQSK can be seen as a version of DualPrompt with adjusted hyper-parameters, and it has nearly the same performance as DualPrompt reported in Tables 1 to 3. Additionally, we jointly train a model using data from all tasks with linear prototypes and prompt tuning as a reference for the upper bound.

## 5.2. Performance Comparison

As shown in Table 1, in the three task settings on ImageNet-R, MQMK achieves SOTA performance. In the 5-task and 10-task splits, MQMK shows no significant performance gap compared to joint training. For the small task split, the continual learning performance with MQMK no longer shows a significant gap compared to traditional joint training with all data. This suggests that the performance on ImageNet-R with the 5-task and 10-task splits may have already approached its oracle. However, on the 20-task split, the improvement with MQMK is relatively small. This may be due to each query generating a subspace, and long-term continual learning leads to an increase in the number of subspaces. Different subspaces might overlap to some extent, making it difficult to perform precise query prompting. Additionally, compared to the high-performing CPrompt and EvoPrompt, MQMK has a clear advantage in terms of forgetting rate. This indicates that MQMK not only achieves higher final performance, but also experiences smaller performance degradation during the learning process. CODA-P has a low forgetting rate, yet its average accuracy is also relatively low. This suggests that CODA-P exhibits overall stability in performance, but its final performance is average.

On CIFAR-100, MQMK also achieves performance close to that of joint training, improving by 3.91% compared to CPrompt, while maintaining a low forgetting rate. On DomainNet, MQMK shows a 2.65% performance improve-

| Number | $A_T$ ( $\uparrow$ ) | Matching Rate ( $\uparrow$ ) |
|--------|----------------------|------------------------------|
| 1      | 62.47                | 36.23                        |
| 4      | 71.20                | 57.82                        |
| 10     | 75.17                | 68.77                        |
| 20     | 78.82                | 77.97                        |

Table 4.  $A_T$  (%) and matching rate (%) under keys of different granularities on 10-task Split ImageNet-R.

ment over CPrompt, along with the lowest forgetting rate. Split-DomainNet is an class-imbalanced dataset, where MQMK achieves 90% accuracy on some tasks, while on tasks with small sample sizes, the accuracy drops to only 60%. The issues of small samples and class imbalance may be the reasons for the poor performance of all continual learning algorithms.

## 5.3. Ablation Study

The components of our method include Multiple Queries (MQ) and Multiple Keys (MK). The corresponding components in existing methods are Single Query (SQ) and Single Key (SK). We discuss the average accuracy and matching rate under four combinations: MQMK, MQSK, SQMK, and SQSK, as illustrated in Figure 4. Using SQSK as the baseline and adding MK,  $A_T$  improves by 2.84% and the matching rate increases by 11.32%. This demonstrates the effectiveness of setting class-level keys for each prompt. By adding MQ,  $A_T$  decreases by 8.13% and the matching rate drops by 8.92%. This is because, under the supervision of cross-entropy, the features of samples from the same class are more clustered, while the features of samples from different classes are more dispersed. The features of multiple classes in a task have already been dispersed, and in this case, SK can no longer represent the feature distribution of all training samples in a task. **When MQ is combined with MK,  $A_T$  increases by 8.21% and the matching rate improves by 32.82%**. This demonstrates that incorporating task-related knowledge significantly enhances retrieval accuracy. In fact, in query-key matching, the improvement of query quality and key quality are complementary. Enhancing both simultaneously has a significant impact on matching rate.

## 5.4. Setting Fine-grained Keys

MQSK leads to a performance decline, whereas MQMK improves performance. This highlights the critical importance of learning reliable keys for distribution representation. Based on MQ, we gradually increase the number of keys from 1 to the number of classes in each task (20 class per task in 10-task Split ImageNet-R), and we report their performance in Table 4. Both SK and MK are special cases of  $N$ -keys. It can be observed that **as the number**

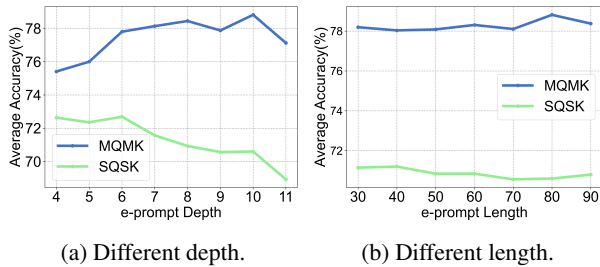


Figure 5. Average accuracy of MQMK and SQSK on the 10-task Split ImageNet-R under different depths and lengths of the e-prompt. (a) The length is fixed at 80, and the depth varies. (b) The depth is fixed at 10, and the length varies.

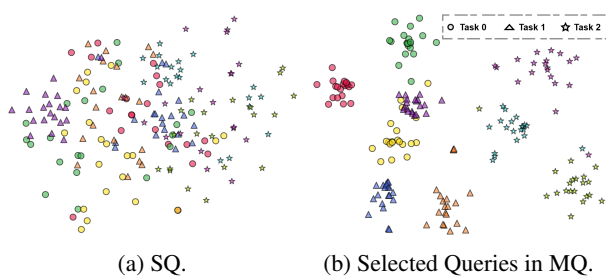


Figure 6. t-SNE (Van der Maaten & Hinton, 2008) visualization of the Queries. The samples come from three classes of three tasks in the 5-task Split Imagenet-R. The shapes represent the sample tasks, and the colors represent the sample categories.

of keys increases, both the matching rate and accuracy improve, and the optimal performance is achieved when the key reaches the class level. Since the smallest granularity of our labels is at the class level, when the number of keys exceeds the number of classes, it becomes difficult to provide appropriate supervisory signals for the keys.

### 5.5. Going Deeper and Longer

As shown in Figure 5, the performance of the MQMK method improves as the e-prompt depth and length increase, reaching its optimal performance of 78.82% when the e-prompt depth is 10 and length is 80. In contrast, the performance of the SQSK method decreases as the prompts go deeper and longer. A possible reason is that increasing the depth and length of the prompt can improve its quality. The higher matching rate of MQMK allows it to effectively utilize the higher-quality prompt, thereby enhancing performance. In contrast, SQSK does not benefit in the same way. This suggests that **an accurate query paradigm can allow the prompt to go deeper and longer, thereby improving model performance.**

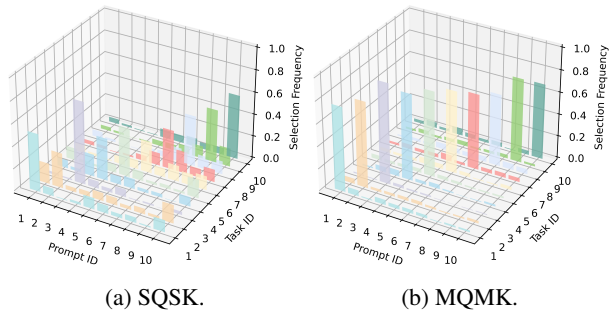


Figure 7. The 3D visualization of specific prompt selection process of MQMK and SQSK on 10-task Split Imagenet-R.

| Dataset    | SQSK  | MQMK  |
|------------|-------|-------|
| ImageNet-R | 45.15 | 77.97 |
| CIFAR-100  | 49.14 | 82.28 |
| DomainNet  | 70.55 | 82.24 |

Table 5. Matching rate (%) on three benchmarks.

### 5.6. Visualization of Queries

We present visualizations of the queries selected by MQ, as well as queries in SQ, as shown in Figure 6. It can be observed that the queries selected by MQ exhibit stronger intra-class cohesion and inter-class separation, indicating that MQ queries are precise and the introduction of prompts is necessary. On the contrary, due to SQ’s reliance solely on ViT’s generalization ability and the lack of task-specific knowledge, the queries of SQ are highly dispersed, resulting in almost failed clustering. Additionally, although the queries show a tendency to cluster by task, the smallest granularity of clustering is at the class level, which indicates the necessity of setting class-level keys.

### 5.7. Prompt Matching Comparison

As shown in Table 5, MQMK improves the matching rate by over 30% compared to SQSK on the challenging CIFAR100 and ImageNet-R. Due to the significant differences in data styles across different domains, SQSK can achieve high performance on DomainNet. To gain a deeper understanding of the prompt selection mechanism, we visualize the specific prompt selection process of MQMK and SQSK, generating two 3D bar charts, as shown in Figure 7. The results indicate that MQMK exhibits a significantly higher probability of selecting the true prompt compared to SQSK.

## 6. Conclusion

To address the issue of low prompt selection accuracy in prompt-based continual learning, we propose the Multiple Queries with Multiple Keys prompt matching paradigm. Multiple Queries achieve precise feature extraction by incor-

porating task-specific knowledge. Multiple Keys, through fine-grained learnable keys, better represent the feature distribution of the training samples. They complement each other, significantly improving the matching rate and performance. However, Multiple Queries introduce a higher inference burden, and exploring ways to accelerate the inference phase with Multiple Queries is a promising direction.

## Impact Statement

This paper presents work whose goal is to advance the field of Machine Learning. There are many potential societal consequences of our work, none which we feel must be specifically highlighted here.

## References

- Belouadah, E., Popescu, A., and Kanellos, I. A comprehensive study of class incremental learning algorithms for visual tasks. *Neural Networks*, 135:38–54, 2021.
- Chaudhry, A., Ranzato, M., Rohrbach, M., and Elhoseiny, M. Efficient lifelong learning with a-gem. *arXiv preprint arXiv:1812.00420*, 2018.
- Chen, T., Kornblith, S., Norouzi, M., and Hinton, G. A simple framework for contrastive learning of visual representations. In *International conference on machine learning*, pp. 1597–1607. PMLR, 2020.
- De Lange, M., Aljundi, R., Masana, M., Parisot, S., Jia, X., Leonardis, A., Slabaugh, G., and Tuytelaars, T. A continual learning survey: Defying forgetting in classification tasks. *IEEE transactions on pattern analysis and machine intelligence*, 44(7):3366–3385, 2021.
- Dosovitskiy, A. An image is worth 16x16 words: Transformers for image recognition at scale. *arXiv preprint arXiv:2010.11929*, 2020.
- Finn, C., Abbeel, P., and Levine, S. Model-agnostic meta-learning for fast adaptation of deep networks. In *International conference on machine learning*, pp. 1126–1135. PMLR, 2017.
- Gao, Z., Cen, J., and Chang, X. Consistent prompting for rehearsal-free continual learning. In *Proceedings of the IEEE/CVF Conference on Computer Vision and Pattern Recognition*, pp. 28463–28473, 2024.
- Graves, A. and Graves, A. Long short-term memory. *Supervised sequence labelling with recurrent neural networks*, pp. 37–45, 2012.
- Hendrycks, D., Basart, S., Mu, N., Kadavath, S., Wang, F., Dorundo, E., Desai, R., Zhu, T., Parajuli, S., Guo, M., et al. The many faces of robustness: A critical analysis of out-of-distribution generalization. In *Proceedings of the IEEE/CVF international conference on computer vision*, pp. 8340–8349, 2021.
- Jia, M., Tang, L., Chen, B.-C., Cardie, C., Belongie, S., Hariharan, B., and Lim, S.-N. Visual prompt tuning. In *European Conference on Computer Vision*, pp. 709–727. Springer, 2022.
- Jung, D., Han, D., Bang, J., and Song, H. Generating instance-level prompts for rehearsal-free continual learning. In *Proceedings of the IEEE/CVF International Conference on Computer Vision*, pp. 11847–11857, 2023.
- Kim, D. and Han, B. On the stability-plasticity dilemma of class-incremental learning. In *Proceedings of the IEEE/CVF Conference on Computer Vision and Pattern Recognition*, pp. 20196–20204, 2023.
- Kingma, D. P. Adam: A method for stochastic optimization. *arXiv preprint arXiv:1412.6980*, 2014.
- Kirkpatrick, J., Pascanu, R., Rabinowitz, N., Veness, J., Desjardins, G., Rusu, A. A., Milan, K., Quan, J., Ramalho, T., Grabska-Barwinska, A., et al. Overcoming catastrophic forgetting in neural networks. *Proceedings of the national academy of sciences*, 114(13):3521–3526, 2017.
- Krizhevsky, A., Hinton, G., et al. Learning multiple layers of features from tiny images. 2009.
- Kurniawan, M. R., Song, X., Ma, Z., He, Y., Gong, Y., Qi, Y., and Wei, X. Evolving parameterized prompt memory for continual learning. In *Proceedings of the AAAI Conference on Artificial Intelligence*, volume 38, pp. 13301–13309, 2024.
- LeCun, Y., Bottou, L., Bengio, Y., and Haffner, P. Gradient-based learning applied to document recognition. *Proceedings of the IEEE*, 86(11):2278–2324, 1998.
- Li, Z. and Hoiem, D. Learning without forgetting. *IEEE transactions on pattern analysis and machine intelligence*, 40(12):2935–2947, 2017.
- Lopez-Paz, D. and Ranzato, M. Gradient episodic memory for continual learning. *Advances in neural information processing systems*, 30, 2017.
- Madaan, D., Yoon, J., Li, Y., Liu, Y., and Hwang, S. J. Representational continuity for unsupervised continual learning. *arXiv preprint arXiv:2110.06976*, 2021.
- McClelland, J. L., McNaughton, B. L., and O’Reilly, R. C. Why there are complementary learning systems in the hippocampus and neocortex: insights from the successes and failures of connectionist models of learning and memory. *Psychological review*, 102(3):419, 1995.

- McCloskey, M. and Cohen, N. J. Catastrophic interference in connectionist networks: The sequential learning problem. In *Psychology of learning and motivation*, volume 24, pp. 109–165. Elsevier, 1989.
- McDonnell, M. D., Gong, D., Parvaneh, A., Abbasnejad, E., and van den Hengel, A. Ranpac: Random projections and pre-trained models for continual learning. *Advances in Neural Information Processing Systems*, 36, 2024.
- Mirzadeh, S. I., Farajtabar, M., Pascanu, R., and Ghasemzadeh, H. Understanding the role of training regimes in continual learning. *Advances in Neural Information Processing Systems*, 33:7308–7320, 2020.
- Nguyen, C. V., Achille, A., Lam, M., Hassner, T., Mahadevan, V., and Soatto, S. Toward understanding catastrophic forgetting in continual learning. *arXiv preprint arXiv:1908.01091*, 2019.
- Peng, X., Bai, Q., Xia, X., Huang, Z., Saenko, K., and Wang, B. Moment matching for multi-source domain adaptation. In *Proceedings of the IEEE/CVF international conference on computer vision*, pp. 1406–1415, 2019.
- Pham, Q., Liu, C., and Hoi, S. Dualnet: Continual learning, fast and slow. *Advances in Neural Information Processing Systems*, 34:16131–16144, 2021.
- Ravi, S. and Larochelle, H. Optimization as a model for few-shot learning. In *International conference on learning representations*, 2017.
- Rebuffi, S.-A., Kolesnikov, A., Sperl, G., and Lampert, C. H. icarl: Incremental classifier and representation learning. In *Proceedings of the IEEE conference on Computer Vision and Pattern Recognition*, pp. 2001–2010, 2017.
- Rumelhart, D. E., Hinton, G. E., and Williams, R. J. Learning representations by back-propagating errors. *nature*, 323(6088):533–536, 1986.
- Russakovsky, O., Deng, J., Su, H., Krause, J., Satheesh, S., Ma, S., Huang, Z., Karpathy, A., Khosla, A., Bernstein, M., et al. Imagenet large scale visual recognition challenge. *International journal of computer vision*, 115: 211–252, 2015.
- Shin, H., Lee, J. K., Kim, J., and Kim, J. Continual learning with deep generative replay. *Advances in neural information processing systems*, 30, 2017.
- Smith, J. S., Karlinsky, L., Gutta, V., Cascante-Bonilla, P., Kim, D., Arbelle, A., Panda, R., Feris, R., and Kira, Z. Coda-prompt: Continual decomposed attention-based prompting for rehearsal-free continual learning. In *Proceedings of the IEEE/CVF Conference on Computer Vision and Pattern Recognition*, pp. 11909–11919, 2023.
- Van der Maaten, L. and Hinton, G. Visualizing data using t-sne. *Journal of machine learning research*, 9(11), 2008.
- Wang, F.-Y., Zhou, D.-W., Ye, H.-J., and Zhan, D.-C. Foster: Feature boosting and compression for class-incremental learning. In *European conference on computer vision*, pp. 398–414. Springer, 2022a.
- Wang, Y., Ma, Z., Huang, Z., Wang, Y., Su, Z., and Hong, X. Isolation and impartial aggregation: A paradigm of incremental learning without interference. In *Proceedings of the AAAI Conference on Artificial Intelligence*, volume 37, pp. 10209–10217, 2023.
- Wang, Z., Zhang, Z., Ebrahimi, S., Sun, R., Zhang, H., Lee, C.-Y., Ren, X., Su, G., Perot, V., Dy, J., et al. Dualprompt: Complementary prompting for rehearsal-free continual learning. In *European Conference on Computer Vision*, pp. 631–648. Springer, 2022b.
- Wang, Z., Zhang, Z., Lee, C.-Y., Zhang, H., Sun, R., Ren, X., Su, G., Perot, V., Dy, J., and Pfister, T. Learning to prompt for continual learning. In *Proceedings of the IEEE/CVF conference on computer vision and pattern recognition*, pp. 139–149, 2022c.
- Yan, S., Xie, J., and He, X. Der: Dynamically expandable representation for class incremental learning. In *Proceedings of the IEEE/CVF conference on computer vision and pattern recognition*, pp. 3014–3023, 2021.
- Zhou, D.-W., Sun, H.-L., Ning, J., Ye, H.-J., and Zhan, D.-C. Continual learning with pre-trained models: A survey. *arXiv preprint arXiv:2401.16386*, 2024.

## A. Key Matching Classifier

| Classifier | FC    | NCM   | KM    |
|------------|-------|-------|-------|
| $A_T$      | 78.82 | 77.25 | 72.27 |

Table 6.  $A_T$  (%) of MQMK using 3 different classifiers on 10-task Split Imagenet-R.

According to Equations (2) and (3), when  $K = 1$ , our method can be interpreted as selecting the key with the highest cosine similarity, and choosing the corresponding prompt. Since MK extends keys to the class level, establishing an identity mapping between keys and classes and directly deriving the classification result upon key selection is more straightforward and worth exploring. We refer to this classifier, which directly classifies based on the selected class-level keys, as the Key Matching (KM) classifier.

We compare the performance of the KM classifier with the Fully Connected (FC) classifier used throughout the experiment and an additional classic prototype-based Nearest Class Mean (NCM) classifier, as shown in Table 6. The performance of the KM classifier was not satisfactory, failing to surpass both the FC and NCM classifiers. Notably, on the 10-task Split ImageNet-R, the matching rate reached 77.97%, as depicted in Table 5. Since the classification accuracy of the KM classifier essentially reflects the accuracy of key matching, while the matching rate represents the accuracy of prompt selection, the gap between them (5.70%) corresponds to the samples where key matching errors occur but the prompt is correctly selected. **The matching rate can be considered a loose upper bound of the KM classifier’s accuracy.** In this task, the matching rate is lower than the FC classifier’s accuracy, which explains why the KM classifier fails to outperform the FC classifier. However, if the matching rate were to improve further, it remains to be explored whether the KM classifier could achieve performance comparable to or even surpassing that of the FC classifier.

## B. Discussion on Computational Costs and Number of Parameters

| Method | Training (GFLOPs) | Inference (GFLOPs) | Learnable Parameters (M) | All Parameters (M) |
|--------|-------------------|--------------------|--------------------------|--------------------|
| SQSK   | 46.92             | 33.22              | 5.63                     | 87.88              |
| MQMK   | 30.56             | 164.10             | 5.70                     | 87.95              |

Table 7. Computational costs and number of parameters of SQSK and MQMK with  $L_e = 40$ ,  $H_e = 6$ ,  $L_g = 5$ ,  $H_g = 2$  on 10-task Split CIFAR-100 dataset.

In Section 4.4, we have discussed the theoretical inference cost of MQMK. In this section, we will discuss the practical computational costs, theoretical training computational costs, and the number of parameters.

**Number of Trainable Parameters.** The total number of parameters in the prompt is  $L_g \times H_g \times D + L_e \times H_e \times D$ , where  $H_g$  represents the number of layers inserted by the g-prompt and  $H_e$  represents the number of layers inserted by the e-prompt. The number of parameters for SK is  $M \times D$ , and the number of parameters for MK is  $|\mathcal{Y}^1 \cup \mathcal{Y}^2 \cup \dots \cup \mathcal{Y}^T| \times D$ . Compared to SQSK, the prompt and classifiers parameters of MQMK remain unchanged, while the key parameters become multiple times the number of categories in each task.

**Training Process.** MQ does not need to be executed. Instead, queries are directly located based on the task  $t$ . Since the prediction and the query use the same features, only one forward and one backward pass through the ViT backbone is required. In contrast, SQSK needs to perform both a query and a prediction with the prompt, which requires two forward passes and one backward pass through the ViT backbone.

**Practical Results.** As shown in Table 7, during the training phase, the computational cost of MQMK is 0.65 times that of SQSK. This is because MQ performs one less forward pass of the ViT. In the inference phase, MQMK’s computational cost is approximately five times that of SQSK. This is due to the multiple forward passes of ViT caused by MQ. The parameter count of MQMK is nearly the same as that of SQSK. Since the number of parameters for the keys is relatively small compared to the prompt, the additional parameter burden introduced by MK is not significant. The practical results align with the theoretical expectations.

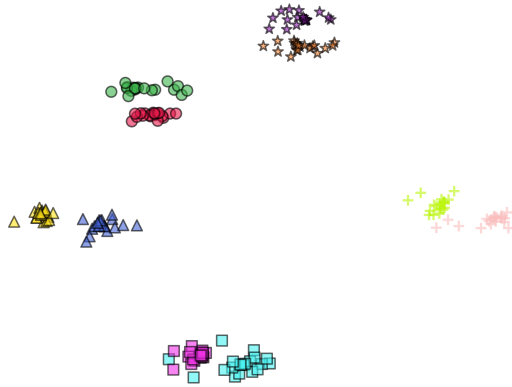


Figure 8. t-SNE visualization of features in perfect match. The samples come from two classes across five tasks in the 5-task Split Imagenet-R. The shapes represent the sample tasks, and the colors represent the sample categories.

### C. Visualization of Features in Perfect Match

In Section 5.6, we have discussed the query visualization of MQ and SQ. In this section, we provide feature visualizations under the condition where the model selects the true prompt for all samples (perfect match), which can be considered an ideal upper bound. As shown in Figure 8, when the true prompt is selected, the discriminability of the features is very strong. Therefore, improving prompt matching rate can significantly enhance performance. Additionally, there is no inherent relationship between classes within the same task. **However, since the same prompt is selected, the features of samples in the same task become very similar. It suggests that different prompts generate different subspaces, and selecting the wrong prompt may cause subspace drift, leading to biased predictions.** This highlights that the selection of the prompt is crucial.

### D. Performance of True and False Prompt in MQMK

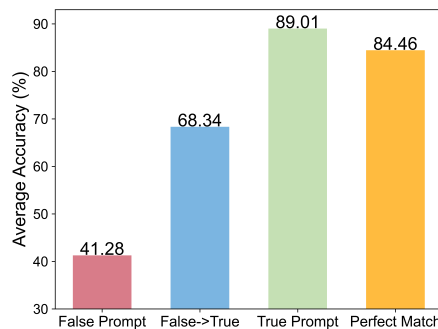


Figure 9. The average accuracy for four scenarios: when MQMK selects False Prompt and True Prompt, when samples initially with False Prompt are manually replaced with True Prompt, and when all samples use True Prompt.

In Section 3.3, we have already discussed the average accuracy of the samples selected with True and False Prompts in SQSK. In this section, we will discuss the situation in MQMK and compare the two scenarios. Compared to SQSK, MQMK has a lower accuracy for the incorrectly selected False Prompt samples. Even when provided with the True Prompt, the performance remains only at 68.34%. **This suggests that MQMK has already matched the more recognizable and straightforward samples, and the remaining samples are inherently difficult to recognize.** Even with the True Prompt, the performance is limited. The samples selected with the True Prompt in MQMK are easier to match and recognize, achieving an accuracy of 89.01%.

| $K$ | $A_T$ ( $\uparrow$ ) | Matching Rate ( $\uparrow$ ) |
|-----|----------------------|------------------------------|
| 1   | 78.82                | 77.97                        |
| 2   | 76.28                | 71.60                        |
| 4   | 72.19                | 59.98                        |
| 10  | 65.10                | 42.13                        |
| 20  | 59.50                | 27.58                        |

Table 8. Average accuracy (%) and matching rate (%) under different  $K$ -category aggregation on 10-task Split Imagenet-R.

## E. Effect of Top- $K$ in Category Aggregation

In previous experiments, we set  $K$  to 1 at all times. Here, we will discuss the performance of aggregating multiple classes and then selecting the prompt. As shown in Table 8, when  $K$  is 1, both performance and matching reach their optimal values. As  $K$  increases, both performance and matching rate decline. This suggests that the classes within the same task are not similar in features, and aggregating the matching scores for a group of classes has a negative effect.

## F. Dataset Introduction

In this section, we introduce three datasets that are used.

- CIFAR-100 is a popular dataset in machine learning, consisting of 100 different classes. It contains 60,000  $32 \times 32$  color images, divided into 50,000 training images and 10,000 test images. Each class contains 600 images, and the categories are diverse, such as animals, vehicles, and household items.
- ImageNet-R is a variant of the ImageNet dataset, designed to evaluate the robustness of machine learning models to transformed or corrupted images. It contains 100,000 images from 200 classes, similar to the original ImageNet, but with images altered by various transformations such as noise, blur, or weather effects. The dataset is useful for testing the generalization and resilience of models to real-world changes in data.
- DomainNet is a large-scale dataset designed to address domain adaptation tasks. It consists of 6 different domains (e.g., real, clipart, painting, and sketch) with a total of over 600,000 images across 345 categories. The dataset is used to evaluate how well models trained on one domain can transfer to others, making it ideal for research on domain adaptation and transfer learning. Since the data in DomainNet is primarily concentrated within 200 classes, we select the 200 classes with the most samples, using the same class-incremental setting and train-test split as in (Gao et al., 2024). Therefore, we compare our results with those reported in their paper on this dataset.